

Dynamic In-Plane Behavior of URM Wall Upgraded with Composites

Mohamed A. Elgwady¹, Pierino Lestuzzi², Marc Badoux³
1,2,3 Swiss Federal Institute of Technology, Lausanne, Switzerland.

Abstract

In many seismically active regions of the world there are large numbers of buildings featuring Un-Reinforced Masonry (URM) bearing walls. Most of these buildings have not been designed for seismic action. Recent earthquakes have shown that many such buildings are seismically vulnerable and should be upgraded. This paper presents preliminary results of laboratory experiments investigating in-plane behavior of URM walls upgraded with composite materials. Half-scale masonry walls were subjected to a series of simulated earthquake motions on an earthquake simulator.

Keywords

Masonry walls, shear walls, earthquakes, dynamic tests, upgrading, composite materials, GFRP.

Introduction

General

Masonry is one of the oldest construction materials. Masonry structures have been in existence since the earliest days of mankind. Clay units have been in use for over 10,000 years. Sun dried bricks were widely used in Babylon, Egypt, Spain, South and North America.

Repeated earthquakes have shown the vulnerability of URM buildings. Improving existing and developing better methods of upgrading existing seismically inadequate buildings is necessary to mitigate the destructive effects of earthquakes. Numerous techniques are available to increase the strength and/or ductility of URM walls. There seems to be a reliability issue with some of the commonly used techniques. Northridge (1994) post-earthquake surveys showed that 450 buildings upgraded before the earthquake failed after the earthquake (Kehoe et al. 1996). The objective of this study is to better understand the behavior of URM walls and to investigate the effectiveness of composite materials as externally bonded strengthening materials.

Failure Modes of URM Walls

Masonry is a non-homogeneous and anisotropic composite structural material, consisting of masonry units and mortar. The behavior of masonry is complex. The accurate prediction of lateral load capacity of URM walls is difficult because of the complex brick block-mortar interaction behavior. The masonry units can be stone, calcium silicate, clay or concrete. This research program deals with clay units.

The main in-plane failure mechanisms of URM walls subjected to earthquake actions are summarized as following:

- **Shear failure:** This takes place when the principal tensile stresses, developed in the wall under the combination of the horizontal and vertical loads, exceed the tensile resistance of masonry materials. Just before the attainment of maximum lateral load, diagonal cracks are developed in the wall. These cracks as shown in *Figure 1(a)* are stair stepped “strong bricks and

weak mortars”. They pass through the bricks in case of “weak bricks and strong mortars”. For high axial load explosive failure may happen.

- **Sliding mode:** In the case of low vertical loads and /or low friction coefficient, which maybe due to poor quality mortar, horizontal cracks in the bed joints will form. These cracks can form a sliding plane extending along the wall length as shown in *Figure 1(b)*.

- **Flexural (rocking) mode:** in case of high moment/shear ratio or improved shear resistance, crushing of the compressed zones at the edge of the wall may happen. Failure is obtained by overturning of the wall as shown in *Figure 1(c)*.

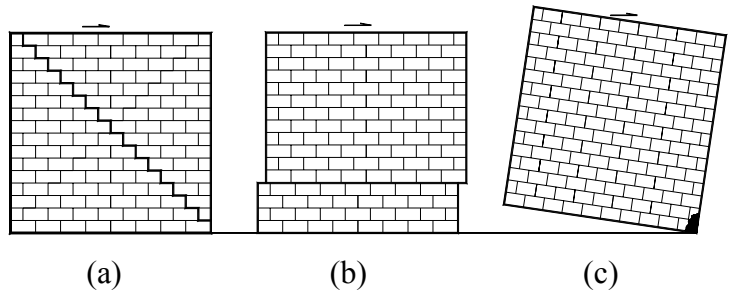


Figure 1. In-Plane Failure Mechanisms Of Laterally Loaded URM Wall, (A) Shear Failure, (B) Sliding Failure, (C) Rocking Failure.

Literature Review

Composite Material

Development of fiber composites began for military and aerospace applications in the first half of the 20th century. Because of their extremely low weight to strength ratio, immunity to corrosion, and their ease of application, composite materials are interesting for seismic upgrading. Experimental tests have shown that in many situations they can be used for seismic upgrading of structures by increasing the lateral resistance and/or ductility of structural elements.

Seismic upgrading of URM walls with bonded composite material has been investigated by several researchers. Focus has been on upgrading to correct inadequate in-plane and/or out-of-plane behavior. Velazquez-Dimas et al. (2000) presented results of an extensive experimental testing program of half scale URM walls upgraded with vertical composite material strips subjected to out-of-plane loading. The upgraded walls resisted pressure from five to twenty four times the weight of the wall and deflected as much as 5% of the wall height. The effectiveness of the Fiber Reinforced Polymers (FRP) in increasing the out-of-plane load-carrying capacity was also examined by Albert et al. (2000), Hamilton et al. (2001), and Hamoush et al. (2001). In all cases, upgrading with composite material has proven to be an efficient technique.

One of the early studies on the use of composites for strengthening URM walls to improve the in-plane capacity was by Schwegler (1995). The effectiveness of this technique was demonstrated through full-scale one story tests. Seven walls were tested under static cyclic loading. The upgrading scheme included Carbon Fiber Reinforced Plastic (CFRP) laminates and wrap (carbon and polyester fibers). The influence of upgrading the walls on one or both sides was investigated. It was found that the lateral resistance and ductility of the walls upgraded on one side only was not significantly lower than the one upgraded on both sides. Also no out-of-plane deformations were noticed for walls strengthened on one side only.

Triantafillou (1998) suggested a simple design model consistent with EC6 for common cases of loading; in-plane bending, out-of-plane bending, and in-plane shear, all combined with axial load. The results obtained from monotonic four-point bending tests on “wallettes” confirm the analysis method for both out-of-plane and in-plane response. The effectiveness of this upgrading technique was confirmed by Reinhorn and Madan (1995), Marshall et al. (1999), and Abrams and Harmon (2001) under static,

static cyclic, pseudo-dynamic, and dynamic loading. In addition, a growing number of field applications using CFRP or Glass Fiber Reinforced Plastic (GFRP) have been reported, including Borgogno (2001), Schwegler and Kelterborn (1998) and Ehsani and Saadatmanesh (1997).

Experimental Program

This experimental program consists of testing 5 URM walls. The test parameters are the aspect ratio, the normal force, the composite material type, and upgrading configurations. The first specimen REFE was a reference specimen for the slender walls. It was tested to the initiation of the rocking mode of failure and then was upgraded with glass fiber. One layer of a glass fiber wrap covered the whole side of the wall and it was retested as specimen WRAP-G. This paper summarizes the experimental results concerning the first and second test specimen.

The third test specimen will be tested to evaluate the shear resistance of the slender walls by using two vertical CFRP laminates at both ends, on one side. This upgrading scheme will force a shear failure and prevent a rocking mode. After testing, the specimen will be upgraded with diagonal glass fiber and retested. Following the first round of wall tests, an additional three walls will be constructed and upgraded. These three walls will include another slender wall and two squat walls.

Description and Construction of the Test Specimens

The test walls are representative of an un-reinforced clay masonry wall in the upper floors of a typical Swiss building of the 1950's as shown in *Figure 2*. Materials were selected such that test specimens would reflect structural characteristics of an older masonry wall. Hollow Clay Masonry (HCM) with relatively weak mortar was used in the construction of test specimens.

Half-scale slender masonry walls were built by experienced masons using half-scale HCM. The walls were constructed in a single wythe, in a running bond pattern with a mortar joint of 5 mm thickness, which is consistent with the half scaled bricks. The nominal dimensions of the walls are 1600 mm height, 1570 mm length, and 75 mm width. Both the head beam and foundation pad were pre-cast concrete. The main geometric features of the constructed walls are illustrated in *Figure 3*.

Bricks

The original HCM unit is 300 X 150 X 190 mm; this resulted in a scaled brick nominally measuring 150 X 75 X 95 mm. These scaled HCM units were produced by a commercial firm.

Mortar

Two types of mortar were used in this experimental program. The first type was a type M2 mortar with cement, lime, and sand in 1:2:9 proportions by volume. This weak type of mortar is representative of older constructions. The maximum sand aggregate size was 3 mm to match the reduced scale brick size. A few joints of the walls required a stronger mortar, so type M15 was used. Type M15 mortar made in a 1:0.25:3 mix of the same cement, hydrated lime and sand. This strong mortar was used for the top and bottom layers of mortar.

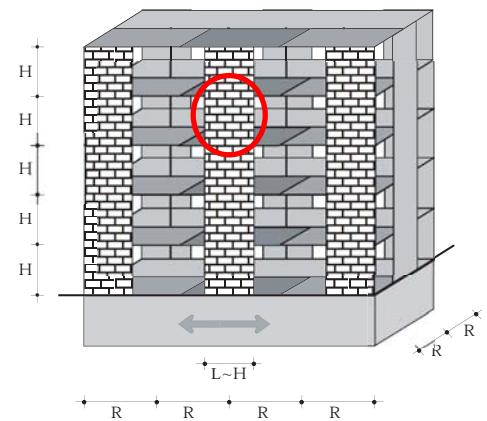


Figure 2. Five-Story Building With External URM Walls And Slender Columns.

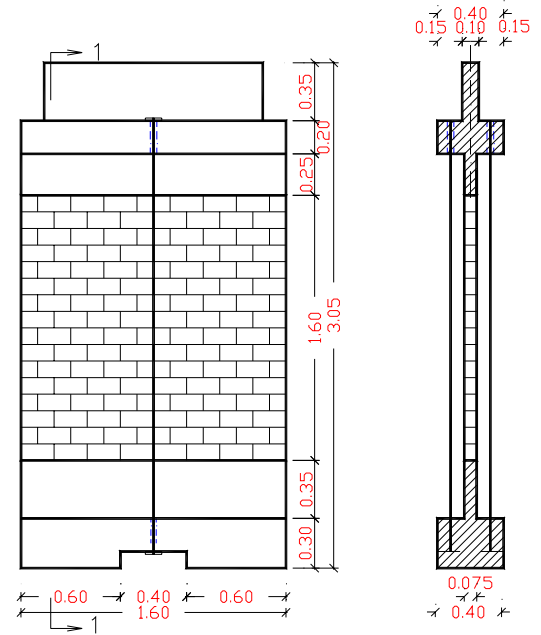
Foundation and Head Beam

The reinforced concrete foundation served the following three functions:

- To be post attached to the earthquake simulator table.
- Provide a lifting element for transportation of the wall via the overhead crane.
- Provide an anchorage surface for the composite material.

The lateral load is transferred through a stiff reinforced concrete head beam simulating a flooring diaphragm. The reinforced concrete pre-cast head beam served the following three functions:

- Apply the prestressing cables.
- Connect the test specimen to the concentrated mass in the test set-up.
- Provide an anchorage surface for the composite material.



Sec (1-1)

Figure 3. Wall Dimensions

Material Properties

Construction Materials

Material properties such as the masonry compressive strength and shear strength will be determined. In this phase a nominal value of 8 MPa is assumed for masonry compressive strength. Preliminary material tests indicate that the characteristic shear strength of masonry under zero compressive stress (f_{v0}) is about 0.1 MPa.

Shove Test

After the dynamic testing of WRAP-G a shove test was performed under a normal force of 0.35 MPa. This test requires the removal of two bricks and a head joint one brick away on the same course, as shown in *Figure 4*. A loading jack is placed in the cavity and the brick between the cavity and the missing head joint is forced towards the missing head joint until shear failure is achieved. The compressive strength of the masonry governed the test. The test was stopped at 35 kN, corresponding to characteristic shear stresses (f_v) of about 1.6 MPa.



Figure 4. Shove Test.

Measuring the Modulus of Elasticity

The modulus of elasticity was measured after wall construction and head beam fixation. Different values of normal forces were applied and the deformations were measured. The maximum normal force applied for each wall was in the order of 35 kN (0.21 MPa). The deformations were measured over the length of the wall. An average value of 4'500 MPa was measured as modulus of elasticity for first wall.

Fibers and Bonding Adhesive

One fiber composite configuration GFRP was evaluated during the first phase of the testing program. The SikaWrap-300G 0/90 fiber system consists of a 290 g/m² cross-ply (i.e. 0/90°) glass fabric. According to manufacture's data it has a maximum tensile strength of 2'400 N/mm², an E-modulus of

70'000 N/mm², and an elongation at rupture of 3%. It was bonded to the wall using two component epoxy Sikadur-330 mixed in a ratio of 4:1 by weight.

Test Set-Up

The walls are tested on a uni-axial earthquake simulator of the Swiss Federal Institute of Technology in Zurich (ETHZ), Switzerland. *Figure 5* illustrates the main components of the test set-up, it includes the following feature:

- The shaking table measures 2m by 1m. The maximum displacement of the simulator from the rest position is $\pm 125\text{mm}$. For safety reasons it was decided to limit the displacements to $\pm 100\text{mm}$.
- The simulator is driven by a 100 kN servo-hydraulic actuator supplied by a 280 bar hydraulic pump with a total capacity of 240 l/min.
- The mass set-up is located to the south of the earthquake simulator. It consists of a steel frame supporting a 12 ton mass consisting of steel bars. The mass is placed on bearing wheels with a low coefficient of friction in the order of 0.5%.
- Two steel beams, are used to guide the specimen at the reinforced concrete head beam level. The friction between the head beam and the steel guides is minimized by using a layer of Teflon connected to the steel beams.

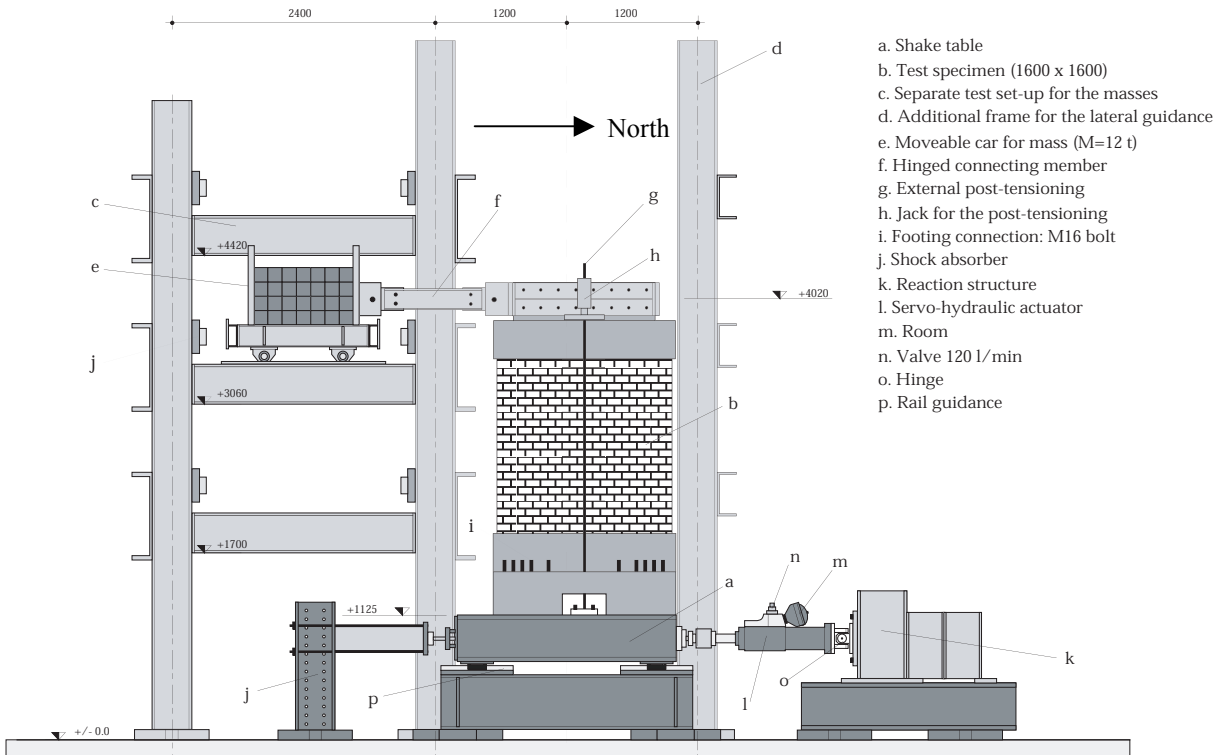


Figure 5. Test Set-Up.

Prior to testing the following steps were done:

- The wall was fixed to the earthquake simulator table through steel bolts.
- The concrete head beam was connected to the mass through a hinged steel member.

Test specimen structural properties

The test walls correspond to an upper story URM wall that has relatively a low normal force and relatively high inertia force. A vertical load representative of the gravity load was applied to the test

specimen. A load of 30 kN was developed via two external prestressing cables. In addition, a vertical load of 11 kN was presented by an own weight of steel elements at wall top, reinforced concrete head beam, and half of masonry panel weight. This normal force corresponded to a stress of 0.35 MPa. The inertia force was provided by the mass was representative of the hatching area in *Figure 1*. Test specimens had boundary conditions similar to a cantilever wall with an effective moment/shear ratio equal to 1.4.

Instrumentation

The specimens were instrumented with several devices as shown in *Figure 6*. Eighteen Linear Variable Displacement Transducers (LVDTs) measured vertical and horizontal displacements and deformations. Three accelerometers were positioned on the mass, on the head beam, and on the table measured the horizontal accelerations. Another two accelerometers were placed at the ends of the head beam measured the vertical acceleration. The table displacement and generated forces were measured using table built in devices. The forces in the prestressing cables were measured using load cells. The force at the head beam was also measured using a load cell. The information red by each device was recorded using a computer controlled data acquisition system. The scanning velocity for each channel was 100 Hz.

Upgrading Procedure

The upgrading of specimen REFE to specimen WRAP-G consisted in the application of a layer of glass fiber fabric on one face of the masonry wall. This was a particularly easy operation. The main steps were as following:

- The surface was roughened by grinding, and then the dust and any loose particles were removed with high air pressure.
- GFRP strips were cut to the desired dimensions.
- The wall surface was coated with a thin layer of two component epoxy
- The GFRP was applied to the wall face by hand and pressed with a roller until homogeneous color was obtained.

The anchorage of externally bonded reinforcement is a common weak point. It is not the goal of the test to test the anchorage of the upgrading system. To ensure that anchorage failure did not occur, steel plates were used to anchor the GFRP to the walls using steel bolts as shown in *Figure 7*.

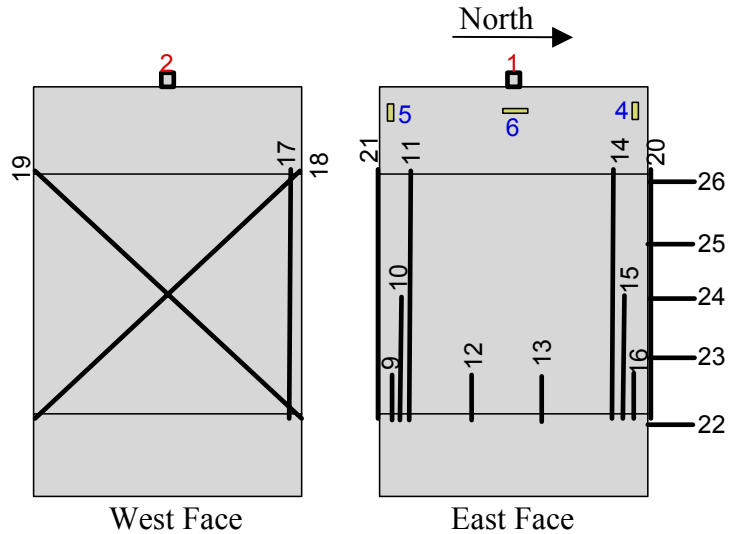


Figure 6. Typical Measurements For Slender Wall.

- Displacement measurements
- ▭ Acceleration measurements
- ▣ Force measurements



Figure 7. Wall Specimen WRAP-G Upgraded On One Side (West Side) Using GFRP.

Loading History

The displacement input for the shaking table was based on artificial acceleration records generated from the spectrum provided by the current Swiss building code for high seismicity zone (3a) and soft soil (type B). Each wall was subjected to an acceleration history of increasing intensity, until failure occurred or a predefined degree of damage was obtained. Each acceleration history had a duration of approximately 15 seconds. The first specimen REFE was subjected to 11 test runs as shown in *Table 1*. An example of generated ground motion, as recorded on the table during testing of REFE is shown in *Figure 8 (a, b)*.

The second specimen WRAP-G was subjected to 24 test runs as summarized in *Table 2*. The first eleven runs were based on the same reference time history as specimen REFE. For the other 13 runs, to avoid the limitation on the maximum stroke of the earthquake simulator; it was decided to use another earthquake with the same maximum acceleration as the first one but with reduced displacement. With the second earthquake it was possible to achieve a higher level of horizontal forces. The second phase of the runs started at an intensity of 100% of the new time history and increased gradually until it achieved an intensity of 230% of the new reference displacement input. An example of generated ground motion, as recorded on the table at the end of testing WRAP-G is shown in *Figure 8 (c, d)*.

Table 1. Loading History of Testing Specimen REFE.

Test Run	Earthquake Type & %	Maximum Prestressing Force (kN)	Maximum H* (kN) (+)	Minimum H* (kN) (-)	Maximum D** (mm) (+)	Minimum D** (mm) (-)
1	UG1 5	30.1	2.5	2.7	0.2	0.2
2	UG1 10	30.2	3.8	4.6	N.A.	N.A.
3	UG1 20	30.3	5.5	7.3	N.A.	N.A.
4	UG1 30	30.7	8.2	7.8	N.A.	N.A.
5	UG1 40	30.8	8.5	11.2	N.A.	N.A.
6	UG1 50	31.7	10.1	12.7	0.9	0.8
7	UG1 60	38.5	13.8	16.7	2.1	2.2
8	UG1 70	69.5	22.7	24.6	7.4	7.7
9	UG1 50-2	35.6	11.2	12.2	N.A.	N.A.
10	UG1 80	58.9	18.3	21.8	N.A.	N.A.
11	UG1 100	89.5	29.7	31.5	12.30	10.60

* Horizontal force at the top of the wall.

** Relative horizontal displacement at the top of the wall.

Experimental Results

In this part, a description of the dynamic behavior of specimen REFE and WRAP-G is discussed.

Test Specimen REFE

The behavior of specimen REFE was dominated by a rocking mode that was initiated by flexural cracking at the bed joints. The final crack pattern for REFE is shown in *Figure 9*. The following was noted during the test:

- Test runs 1-5 (40%) caused no visible damage.
- Test run 6 (50%) produced a small horizontal crack in the bed joint between the second and the third course near the bottom south of the wall.

Table 2. Loading History of Testing Specimen WRAP-G

Test Run	Earthquake Type & %	Maximum Prestressing Force (kN)	Maximum H* (+) (kN)	Minimum H* (-) (kN)	Maximum D** (+) mm	Minimum D** (-) mm
1	UG1 10	30.0	2.9	3.0	0.2	0.2
2	UG1 20	30.1	4.4	4.7	N.A.	N.A.
3	UG1 30	30.2	5.8	6.6	N.A.	N.A.
4	UG1 40	30.3	6.7	6.6	N.A.	N.A.
5	UG1 50	30.4	8.2	8.6	N.A.	N.A.
6	UG1 60	30.5	9.3	9.4	0.5	0.6
7	UG1 70	30.7	10.7	11.2	0.7	0.6
8	UG1 80	30.8	11.7	12.9	0.8	0.7
9	UG1 90	32.5	13.2	14.5	0.8	0.8
10	UG1 100	32.1	14.0	15.6	0.9	0.8
11	UG1 120	31.6	16.8	18.5	1.1	1.0
12	UG1R 100	31.7	18.2	19.2	1.2	1.1
13	UG1R 120	32.7	22.5	21.9	1.7	1.4
14	UG1R 130	33.3	24.5	23.2	1.8	1.5
15	UG1R 140	33.8	26.2	24.3	2.0	1.7
16	UG1R 150	34.1	26.9	24.7	1.9	1.8
17	UG1R 160	34.1	27.3	23.8	2.0	1.8
18	UG1R 170	34.1	27.6	22.9	2.0	1.8
19	UG1R 180	33.4	24.1	23.7	N.A.	N.A.
20	UG1R 190	39.8	36.9	40.0	3.7	3.5
21	UG1R 200	45.0	41.9	45.3	7.26	5.19
22	UG1R 210	50.6	43.8	48.8	7.40	5.98
23	UG1R 220	55.4	45.0	50.3	7.7	6.80
24	UG1R 230	87.5	49.5	65.0	12.5	16.1

* Horizontal force at the top of the wall.

** Relative horizontal displacement at the top of the wall.

- Test run 7 (60%), the previous crack was extended slightly into the north part of the wall and the normal force started to increase.
- The greatest amount of cracking occurred during test run 8 (70%). A new crack appeared in the north part of the wall in the bed joint between the third and fourth course. This new crack extended till it was connected to the old one. At this point there was no continuity left between the upper part and the lower part of the wall. However, the rest of the wall above and under the bed joint did not experience any observable damage or large cracking.
- During test runs 8 to 10 the wall displayed a characteristic rocking behavior and the normal force increased many times because of the large opening of the “rocking crack”. These runs produced no additional large cracking. Only two small cracks appeared in the brick at the first and third course. Very limited spalling of masonry cover at the third course was observed
- At the end of the test, wall REFE showed little damage. As shown in *Figure 10* no visible damage or crushing to the brick units or mortar was observed. The test was interrupted in order to preserve the specimen for the subsequent upgraded wall test.

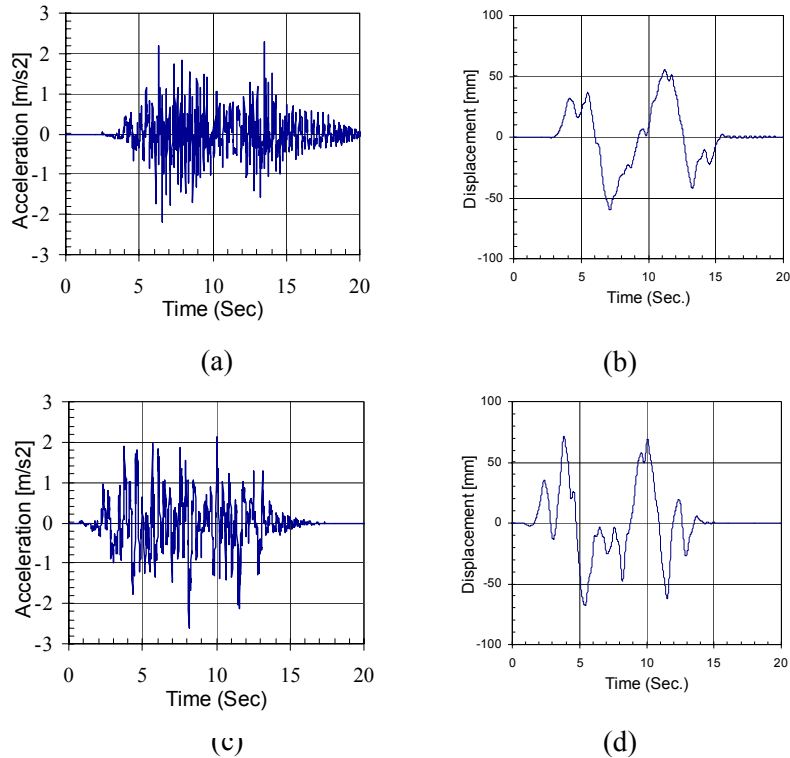


Figure 8. Recorded Earthquake At The End Of Testing Specimen REFE (a And b) And WRAP-G (c And d)

Test Specimen WRAP-G

Specimen REFE was upgraded and tested as WRAP-G. The mode of failure was rocking mode and the ultimate horizontal load for specimen WRAP-G was attained when the masonry at the wall toes crushed in compression. The final crack pattern for WRAP-G is shown in *Figure 11*. The following was noted during the test:

- Test runs 1 to 18 produced no visible damage to WRAP-G.
- The delamination process began in a few points during test run 14. This delamination was visible in the form of white spots on the wrap.
- During test run 19, both the horizontal force and the prestressing force decreased slightly. No visible damage was noticed.
- During test runs 20 to 23 both of the horizontal force and the prestressing force increased rapidly.
- During test run 24 the wall started to rock at the base. This rocking was accompanied with crushing of the masonry at the wall corners. The wall failed under a combination of “local buckling” and tear at the wall corner as shown in *Figure 12*.

Discussion Of The Behavior Of Walls

The walls had a moment to shear ratio of 1.4. Both of the specimens displayed a rocking mode of failure. The reference specimen REFE rocked developing a single crack between the second and third brick course. Upgraded wall WRAP-G rocked at the wall base. As large flexural cracks formed, the prestressing force increased. This increase in normal force influenced the wall resistance. The maximum

prestressing force was similar at the test end of both specimens. On the basis of the observed and recorded behavior the following comments can be made.

Test Specimen REFE

- For a vertical prestressing force of about 33 kN (total vertical force at the wall base of about 45 kN) the lateral resistance of the wall was 15 kN (test run 6 to 7). A doubling of the lateral resistance (to 31.5 kN) was measured when the prestressing force tripled (to about 90 kN).
- The test wall REFE was able to withstand displacements several times greater than the cracking displacements without significant damage, even after numerous rocking cycles. This confirms that rocking can be classified as a stable and favorable post cracking behavior for URM walls.
- After formation of the full-length horizontal crack, no new horizontal cracks appeared in spite of the very weak mortar used. Therefore, minimum mortar strength seems sufficient to maintain the wall integrity during repeated rocking cycles.
- *Figure 13* shows the horizontal force versus the wall top deflection during test run 11. The hysteretic curves show a clear bilinear behavior with a soften part when the rocking crack is open. The hysteretic loops show noticeable pinching and indicate limited energy dissipation.

Test Specimen WRAP-G

- For a vertical prestressing force of about 33 kN (total vertical force at the wall base of about 45 kN) The lateral resistance of the wall was 27 kN (test run 18 to 19). A doubling of the lateral resistance (to about 65 kN) was measured when the prestressing force tripled (to about 87.5 kN).
- The upgrading caused a shifting of the rocking plane to the wall base.
- Generally, the presence of the GFRP system prevented development of cracks through the wall panel itself, i.e. the wall didn't experience any damage until masonry crushing at the bottom corners. Rupture of the GFRP at the wall base was not observed prior to the compression failure.
- A common method for predicting the flexural capacity of structural elements is the use of elastic-plastic (stress block) approach. It was used to predict the horizontal strength of wall WRAP-G. There was a good agreement between experimental and predicted ultimate load.
- As was expected no out-of-plane deformations of the upgraded wall was observed. Even though it was upgraded on one side only.
- Wall WRAP-G exhibited a stable hysteretic force displacement relationship as shown in *Figure 14*.

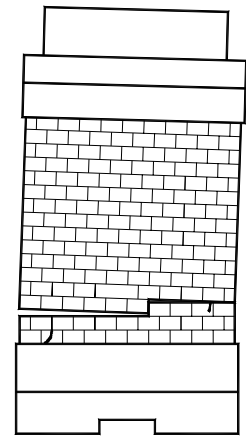


Figure 9. Cracking Pattern Observed In Wall REFE.



Figure 10. Specimen REFE After Testing

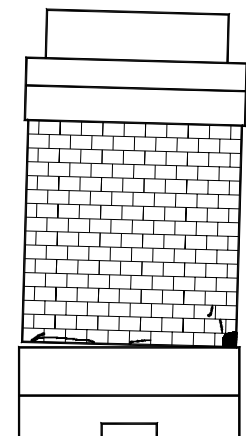


Figure 11. Observed Crack Pattern For Wall WRAP-G



(a)



(b)

Figure 12. (a) Failure Of The GFRP Fabric At The Base Of The Masonry Wall And (b) Crushing Of The Masonry At The Wall Toe.

Comparison of hysteretic behavior

- The hysteretic force displacement relationship for both walls at the test end is shown in *Figure 15*. An improved performance was observed in the upgraded specimen. The lateral resistance is doubled from 31.5 to 65 kN. Energy dissipation remain small in both cases.
- The stiffness of specimen WRAP-G, beyond 2mm lateral displacement was superior to that of specimen REFE.

Summary

Half-scale URM square panel test walls were subjected to a series of simulated earthquake motions on an earthquake simulator. The first wall was a reference specimen. After limited rocking tests, it was upgraded using one layer GFRP and tested again. Within the scope of this study, the following preliminary conclusions can be made:

- This test confirms that wall rocking can be a stable nonlinear behavior in URM walls when no out of plane response occurs.
- The experimental test has demonstrated that the described upgrading technique is a promising. The lateral resistance of the upgraded specimen was enhanced by a factor of about two compared to the non-upgraded one.
- The upgrading postponed the onset of nonlinear behavior and the associated local deformations. The earthquake causing rocking for specimen WRAP-G was three times more in acceleration than specimen REFE. This is a very significant improvement from a “continued operation” limit state point of view.

Acknowledgments

The financial support provided by CTI, with the SIKA Company is gratefully acknowledged. Appreciation is also extended to The Swiss Federal Institute of Technology in Zurich (ETHZ), Switzerland.

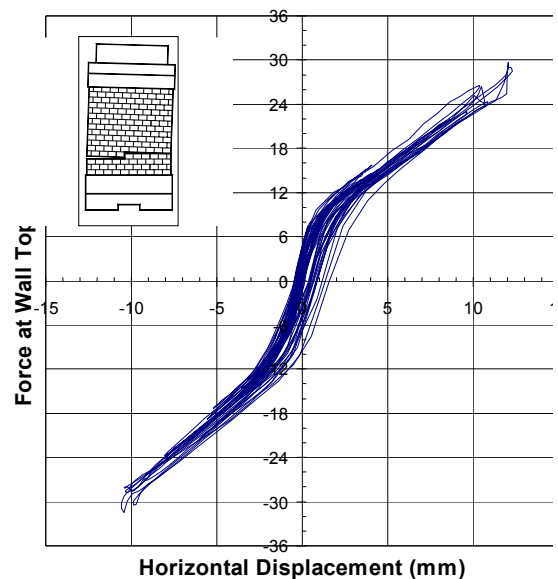


Figure 13. Load Versus Horizontal Deflection At Wall Top During Test Run 11 For Wall REFE.

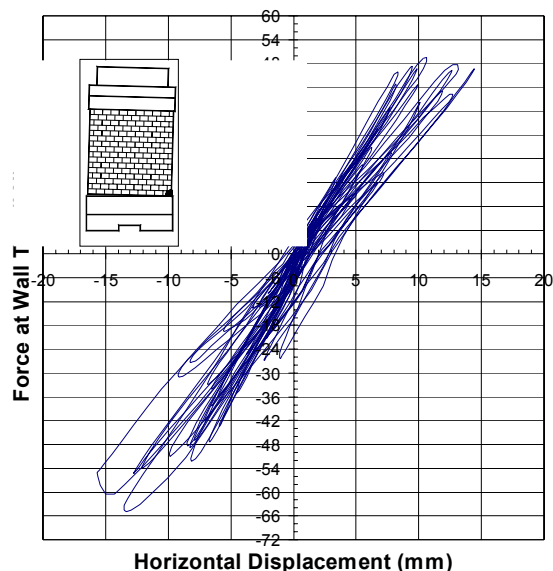


Figure 14. Load Versus Horizontal Deflection At Wall Top During Test Run 24 For Wall WRAP-G.

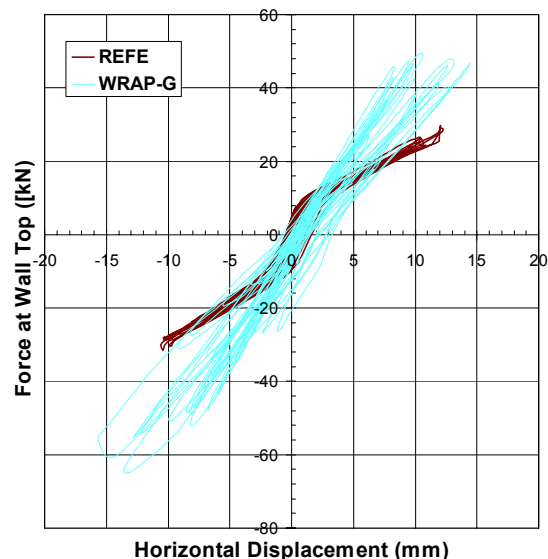


Figure 15. Load Versus Horizontal Deflection At Wall Top At The Test End For Wall REFE And Wall WRAP-G.

References

1. Abrams, D.; Harmon; (2000), Mid America Earthquake Center, Project ST-6, Internet Site.
2. Albert, I. Micheal, Elwi, E. Alaa; and Cheng, J. J. Roger, (2001), "Strengthening of Unreinforced Masonry Walls Using FRPs", *J. Comp. For Constr.*, ASCE, Vol. 5, No. 2, 76-84.
3. Borgogno, W., (2001), "Earthquake Retrofit of a Low Rise Building –Composite Fiber Plates for Strengthening of Masonry Walls and Their Anchorage", 20th EAEE Regional Earthquake Engng. Seminar, Sion, 121-122
4. Hamilton III, H. R.; and Dolan, C. W, (2001), "Flexural Capacity of Glass FRP Strengthened Concrete Masonry Walls", *J. Comp. For Constr.*, ASCE, Vol. 5, No. 3, 170-178.
5. Hamoush, A. Sameer; McGinley, W. Marc; Mlakar, Paul; Scott, David; and Murray, Kenneth, (2001), "Out-of-Plane Strengthening of Masonry Walls with Reinforced Composites", *J. Comp. For Constr.*, ASCE, Vol. 5, No. 3, 1392-145.
6. Kehoe, B. E., (1996), "Performance of Retrofitted Unreinforced Masonry Buildings", 11th WCEE, Acapulco, Mexico, Paper No. 1417.
7. Marshall, Jr.; Sweeney, S. C.; and Trovillion; J. C., (1999), "Seismic Rehabilitation of Unreinforced Masonry Walls", *ACI, SP 188-26*, 287-295.
8. Reinhorn, A. M.; Maden, A., (1995), "Evaluation of TYFO-W Fiber Wrap System for in Plane Strengthening of Masonry Walls", Rep. No. 95-0002, Dept. of civil Eng., State University of New York at Buffalo.
9. Schwegler, G., (1994), "Masonry Construction Strengthened with Fiber Composites in Seismically Endangered Zones", 10th Europe. Conf. Earthquake Engng., Vienna, 2299-2303.
10. Schwegler, G.; and Kelterborn, P., (1996), "Earthquake Resistance of Masonry structures strengthened with Fiber Composites", 11th WCEE, Acapulco, Mexico, Paper No. 1460.
11. Triantafyllou, C. Thanasisw, (1998), "Strengthening of Masonry Structures Using Epoxy-Bonded FRP Laminates", *J. Comp. For Constr.*, ASCE, Vol. 2, No. 2, 96-104.
12. Velazquez-Dimas, J. I.; and Ehsani, M. R., (2000), "Modeling Out-of-Plane Behavior of URM Walls Upgraded with Fiber Composites", *J. Comp. For Constr.*, ASCE, Vol. 4, No. 4, 172-181.
13. Ehsani, M. R.; and Saadatmanesh, H., (1997), "Fiber Composites: An Economical Alternative For Retrofitting Earthquake-Damaged Precast-Concrete Walls", *Earthq. Spec.*, Vol. 13, No. 2, 225-241.